Hindawi
Journal of Sensors
Volume 2022, Article ID 2482638, 13 pages
https://doi.org/10.1155/2022/2482638

Research Article

Model Analysis of Sandstone Tunnel Cracking Based on Fracture Mechanics Theory and Sensor Testing Technology Research

Hu Jin, Bo Gao, and Yusheng Shen

Key Laboratory of Transportation Tunnel Engineering, MOE, Southwest Jiaotong University, Sichuan Chengdu 610031, China

Correspondence should be addressed to Hu Jin; jinhu@home.swjtu.edu.cn

Received 22 November 2021; Revised 14 January 2022; Accepted 21 January 2022; Published 14 February 2022

Academic Editor: Gengxin Sun

In this paper, we survey sandstone tunnels using sensor testing technology and conduct an in-depth analysis and research on the model of sandstone tunnel cracking based on the theory of fracture mechanics. This paper systematically investigates the static mechanical properties, energy evolution and distribution law, acoustic emission monitoring, and digital image correlation methods of intact and jointed rock chamber enclosures (including parallel jointed rock chamber enclosures and cross jointed rock chamber enclosures) under static loads, based on physical simulation test methods and combined with other technical means such as acoustic emission monitoring and digital image correlation methods. In this paper, the effects of parallel and cross-joint angles on the static mechanical properties, energy evolution and distribution, acoustic emission variability, progressive destabilization, and their mechanisms are compared and analyzed. This paper takes fiber Bragg grating (FBG) sensing theory and technology research as a breakthrough, relies on major underground engineering geohazard model tests, and proposes a grating spectral reconstruction theory based on the wavelength position constraint of the spectral center and its improvement based on an in-depth analysis of the influence of fiber grating intrinsic parameters and strain distribution on the reflection spectral properties. Based on an in-depth analysis of the influence of spectral center wavelength location and strain distribution on the reflectance spectral properties, we propose the grating spectral reconstruction theory based on the spectral center wavelength location constraint and its improved genetic algorithm optimization method; realize the fast and accurate identification and rejection of the melancholy effect of fiber grating; propose the sensor numerical simulation optimization design method; develop the high sensitivity seepage pressure sensor, new strain sensor, target flow sensor, microdisplacement sensor, and multipoint displacement sensor; and build a large capacity, multi-parameter fiber grating real-time monitoring network.

1. Introduction

After entering the 21st century, with the implementation of the modernization strategy and continuous deepening, the national investment in some important fields related to the national economy and people's livelihood has increased greatly, and the fields of transportation and civil engineering, water conservancy, and hydropower, mineral resources, electric power and energy, aerospace, machinery, and chemical industry have ushered in an unprecedented leap forward, which has brought great opportunities for the development and progress of science and technology in various fields [1]. However, at the same time, engineering disasters and geological disasters, as well as major production safety accidents, have become the main challenges for the construction and development of various fields, which are very likely to cause serious casualties, huge economic losses, and bad social impacts. Especially in the field of underground engineering, the frequent occurrence of geological disasters has become a bottleneck restricting the construction of underground engineering [2]. After entering the 21st century, with the implementation and continuous deepening of the modernization strategy, the state's investment in some important areas related to the national economy and people's livelihood has increased significantly. The fields of transportation and civil engineering, water conservancy and hydropower, mineral resources, electric energy, aerospace, machinery, and chemical industries are all welcome. An unprecedented leap-forward development

has brought huge opportunities for the development and progress of science and technology in various fields. In mines, sudden water accidents have become a major disaster that endangers mine safety, with more than 250 pairs of mines flooded in the past 20 years and direct economic losses amounting to hundreds of millions of yuan, and 285 of the country's key coal mines are threatened by water hazards, accounting for 47.5% of the total. To deal with water hazards in coal mines, discharges 5.6 billion m^3 of mine water every year, causing serious water depletion and environmental damage. In the field of transportation and hydropower, as the construction of water conservancy and hydropower projects and railway and highway projects have shifted their focus to the western mountainous areas under complex terrain and geological conditions, many tunnel caves with significant characteristics such as "large depth of burial, long cave lines, strong karst, high water pressure, high risk of disasters and construction difficulties" have emerged, and the complex hydrogeological conditions and sudden water, landslides, and other major geological hazards are a major concern. The complex hydrogeological conditions and major geological hazards such as sudden water and landslides are considered world-class engineering problems [3]. At the same time, engineering catastrophes, geological disasters, and major production safety accidents have become the main challenges for the construction and development of various fields in our country, which can easily cause serious casualties, huge economic losses, and bad social impacts.

The twenty-first century is the century of underground space. The development and utilization of underground space are an inevitable choice for human social development, economic construction, and the strategic needs of national security. In recent years, the construction of mining, traffic tunnels, water conservancy, hydropower, oil caverns, nuclear waste disposal, carbon dioxide geological storage, and national defence is developing at an unprecedented speed, and the underground chambers (such as tunnels, tunnels, mine tunnels, and shafts) are "long, large, deep and group." The number of "long," "large," "deep," and "massed" underground chambers (e.g., tunnels, tunnels, mine tunnels, and shafts) has increased to an unprecedented scale. With the introduction of the "deep earth" science strategy, it is predicted that the construction of large-scale, high-depth rockwork will become the norm, and underground engineering will become increasingly complex [4]. At the same time, the problems of strong disturbances and high ground stresses in rockwork chambers are becoming more serious, posing a significant challenge to the analysis and maintenance of the stability of the refuge envelope. The design and safe operation of underground chambers in rock engineering is directly dependent on an in-depth study of the deformation and damage characteristics and destabilization mechanisms of the project rock mass. The excavation of an underground chamber disrupts the original equilibrium stress state of the rock mass, causing a series of complex mechanical response behaviours associated with stress redistribution in the surrounding rock mass. In the fields of transportation and hydropower, as the focus of construction of water conservancy and hydropower projects and railway and highway projects has shifted to the western mountainous areas under complex terrain and geological conditions, a number of large buried depths, long tunnel lines, strong karst, high water pressure, tunnels with distinctive features such as high disaster risk and high construction difficulty, complex hydrogeological conditions, and major geological disasters such as water inrush and landslides can be regarded as world-class engineering problems. The deformation of the refuge rock is characterized by the emergence and expansion of cracks and the interpenetration of multiple cracks, which in turn leads to varying degrees of damage at the excavation face, ranging from flaking and spalling to major inward extrusion [5]. The present stage of the construction of infrastructure projects has avoided the contact between the engineering body and the geological body, of which the geological body is mainly rocking, soil, and the engineering body is the most common concrete. The application of concrete has been an essential part of engineering construction at this stage. Traditional support theory, design method, and construction technology are more based on normal temperature conditions, or not recommended for construction in low temperature, but cold zone engineering construction inevitably to accept the cold zone low-temperature impact, the traditional design method has been unable to meet the cold zone engineering construction needs [6]. As the frontier technology of modern science and technology, sensing technology, computer technology, and communication technology are considered as the three technical pillars of modern information technology and become the high point of human competition for high-tech technology in the 21st century.

2. Related Works

For the freeze-thaw damage of porous rocks and concrete, the theory of volume expansion was proposed in 1909. This theory suggests that water undergoes about 9% volume expansion during freezing. In confined pore spaces, damage can occur due to ice pressure that breaks the skeleton of the rock particles. However, the volume expansion theory has been questioned by other scholars as rocks under natural conditions are more likely to have connected pores [7]. The hydrostatic pressure theory was proposed in the study of concrete freeze-thaw damage due to the connectivity of pores within the rock. In addition, in the 1930s, it was found that unfrozen water in the soil migrates towards the ice surface, which in turn continuously forms subcondensed ice at the ice surface. It has also been found that water condensation ice can also form in frost-prone rocks with small mineral grains. The phenomenon of pore water freezing in different types of rocks was studied, and it was found that some of the pore water did not produce freezing at low temperatures [8]. It was found that the unfrozen water phenomenon is mainly due to the formation of an unfrozen water film between the ice and the rock skeleton, and the unfrozen water keeps migrating to the unfrozen water film during the freezing process [9]. With the proposal of the "deep ground" scientific strategy, it can be predicted that in the future, large-scale, high-burial rock mass engineering construction

will become normal, and underground engineering will become increasingly complicated. At the same time, the problems of strong disturbance and high ground stress faced by chambers in rock mass engineering have become more serious, which brings great challenges to the stability analysis and maintenance of chamber surrounding rocks. The existence of adsorption of unfrozen water in rocks to ice crystals was subsequently confirmed. Many studies have been done by related scholars on water migration under the freeze-thaw action of rocks. From the previous studies, it is known that the migration of water inside the rock or concrete under the action of freeze-thaw cycles can cause its local damage fracture phenomenon. For the rock-concrete binary, the interface is usually a naturally weak surface with low tensile strength and is therefore susceptible to moisture migration, which can lead to unpredicted freeze-thaw damage. Furthermore, due to the peculiarities of the interface presence, the mode of moisture migration behavior is not well established [10]. Thus, the study of moisture migration and damage debonding at the rock-concrete binary interface under freeze-thaw action is a good academic prospect in terms of binary interface bonding in cold regions.

There are two main branches of fiber optic sensing technology, which are fully distributed fiber optic sensing technology based on Raman scattering or Brillouin scattering and quasi-distributed fiber optic sensing technology based on fiber grating. The fully distributed fiber optic sensing technology uses an optical fiber as an extended sensitive element, and any unit on the fiber is both a sensitive unit and an information transmission channel for other sensitive units, which fundamentally breaks the traditional single point measurement mode limitation, but its disadvantage is that due to the extremely fast propagation speed of light, the technology requires a very high signal acquisition speed, and the signal processing usually takes a section of the optical fiber multiple acquisitions signals [11]. The average value of the signals collected on a section of the fiber is usually taken, which makes the spatial resolution low and therefore not suitable for the detection of abrupt fields; at the same time, the Raman and Brillouin scattering signals are extremely weak, so the signal processing is very tedious, which also makes the price of the sensing system high, which seriously limits the further application of the technology. The most widely used is based on fiber grating quasidistributed fiber optic sensing technology, because the fiber grating is a reflective optical device, able to produce several different center wavelength grating in an optical fiber, and time division multiplexing and wavelength division multiplexing technology combined to form a sensor array, suitable for buried in the material and structure or mounted on its surface, to achieve quasidistributed temperature, pressure, strain, and displacement parameters [12]. They are suitable for quasidistributed measurements of parameters such as temperature, pressure, strain, and displacement, either buried inside or mounted on the surface of materials and structures. The deformation and failure of the surrounding rock of the chamber are mainly manifested by the initiation and propagation of cracks and the interpenetration of multiple cracks, which leads to different degrees of damage to the rock mass of the excavation surface,such as extrusion and large deformation. At this stage, basic engineering construction cannot avoid the contact between engineering bodies and geological bodies. The geological bodies are mainly rock and soil bodies, and concrete is the most common form of engineering bodies.

In the field of current measurement, current sensors based on the tunnel magnetoresistance (TMR) effect have also received extensive attention. The designed current sensor with Wheatstone bridge structure is based on a magneto resistive element with magnetic tunnel junction structure, the current sensor has a DC measurement range of ±30 A, the sensitivity of 9.8 mV/A, and -3 dB bandwidth of 200 kHz for AC sensor, and the temperature coefficient of sensitivity is 0.031%/°C under different temperature tests, which is lower than the giant magnetoresistance current sensor based on spin valve structure [13]. Related scholars have applied TMR current sensors to current detection in integrated circuits to achieve current measurements from μA to mA levels, but there are strict requirements on the geometric design of the sensor chip, fabrication process, and testing methods. The TMR current sensor has been explored for high-frequency current testing, achieving a maximum current of 2.1 kA at operating frequency with a sensitivity of 35 μV/A and a nonlinearity of 1.5%. The application of TMR current sensor in the leakage current detection of high-voltage bushings is explored; the jointly developed TMR sensing chip shows good performance in the leakage current detection test of ZnO valve piece in surge protector, which provides a new idea and method for the noncontact measurement of leakage current of high-voltage devices [14].

2.1. Analysis of Sandstone Tunnel Cracking Model Based on Fracture Mechanics Theory. According to the different stress states of the geotechnical body, the stress path can be divided into two mechanical states, loading, and unloading. According to the subdivision of loading rate and unloading rate, it can be further divided into various combinations of loading and unloading. The mechanical properties of the rock body vary with different combinations of mechanical states. For rock loading or unloading, the difference in the process of stress change leads to the same transformation of total energy [15]. The loading damage process is equivalent to the external energy input to the rock mass, while for the rock mass with a certain ground stress field, during which there is residual strain energy, the excavation, and unloading of the rock mass is a process of energy release, resulting in changes in the mechanical properties of the rock mass and its integrity. In the study of practical problems, the actual stress conditions of the rock project should be distinguished, and different rock stress-strain paths should be selected for analysis according to the specific stress conditions. The biggest difference between rock loading and unloading is shown by the different stress paths. Fully distributed optical fiber sensing technology uses an optical fiber as an extended sensitive element. Any unit on the optical fiber is both a sensitive unit and an information transmission channel for other sensitive units. It fundamentally breaks through the limitation of the traditional single-point measurement mode. The

disadvantage is that due to the extremely fast propagation speed of light, this technology requires extremely high signal acquisition speed, and in signal processing, the average value of multiple acquisition signals on a piece of optical fiber is usually taken to make its spatial resolution low, so it is not suitable for use. For the detection of mutation field, if $\sigma 3$ remains unchanged and keeps increasing the maximum principal stress $\sigma 1$, i.e., when changing from B $\longrightarrow$ B1 $\longrightarrow$ B2 $\longrightarrow$ B3, the Mohr stress circle also keeps increasing, i.e., the partial stress is a gradually increasing process, so with the increase of load, the partial stress keeps increasing until the rock body is damaged. If the rock is unloaded, if $\sigma 1$ remains unchanged, as $\sigma 3$ decreases from A $\longrightarrow$ A1 $\longrightarrow$ A 2 $\longrightarrow$ A3, the Mohr stress circle becomes larger in the reverse direction, and even $\sigma 3 < 0$ may occur, i.e., it changes from the compressed state to the tensile state, which eventually leads to the destruction of the rock mass. If both $\sigma 1$ and $\sigma 3$ are changed during loading or unloading, more complex stress-strain states will be evolved. As shown in Figure 1, the Mohr stress circle is displayed.

According to the classification of the structural form of rock engineering, open-pit mine slope engineering belongs to the ground engineering in rock engineering, which is different from another ground engineering because of its special mechanical nature and conditions. When the open pit slope is excavated and exposed, the original ground stress equilibrium is broken, and the rock slope has the tendency to move to the stable state, at this time, its mechanical state is mainly manifested as unloading, and at this time, if the construction of external discharge field is carried out along the help, the vertical compressive stress is produced on the slope, that is, the rock slope is adjusted from the original ground stress equilibrium state to the stress state of tension and compression. Therefore, the analysis of hand-excavated slopes should not ignore the damage and deformation caused by unloading [16]. At present, the most widely used is the quasidistributed optical fiber sensing technology based on fiber gratings. Because fiber gratings are reflective optical devices, multiple gratings with different central wavelengths can be continuously produced in a single fiber. The multiplexing technology is combined to form a sensor array, which is suitable for being embedded in materials and structures or mounted on the surface, and realizing quasidistributed measurement of parameters such as temperature, pressure, strain, and displacement.

Conventional structural mechanics theory usually treats structural materials as isotropic homogeneous materials, but materials can have cracks or crack-like defects due to their own or external reasons, and crack-containing structures may be damaged when the stress of the member is far from reaching the yield stress, and such damage shows that it is difficult to accurately evaluate the performance and service state of a structure by using conventional mechanical theory analysis alone, no matter how accurately it is done. Therefore, scholars have proposed fracture mechanics on this basis. Fracture mechanics is an important theoretical basis for analyzing the strength and life prediction of engineering materials and components, and it is a new discipline to study the equilibrium, expansion, and destabilization laws of cracks and their strength of components containing cracks under the action of external forces. In online elastic fracture mechanics, concrete is no longer considered as a damage-free structure, but as a crack, model to study the conditions of crack extension and the process of crack extension, and its main mechanical parameter characterizing crack extension is the strength factor K, which represents the stress field at the crack tip and can describe cracking more accurately. Fracture mechanics is widely used in the study of crack extension in concrete.

Crack fracture criteria can be divided into two categories depending on whether the crack extends along the crack direction or not: single type crack fracture criteria and compound type crack fracture criteria. The essential difference between composite crack and single type crack is that the cracking direction no longer expands along the original crack surface, but has a certain angle with it. So composite cracks need to determine the angle of crack expansion based on a single crack. There are three commonly accepted ones: (1) the maximum energy release rate criterion, (2) the minimum strain energy density criterion, and (3) the maximum circumferential stress criterion. The three fracture criteria are based on energy-based parameters, strain-parameter, and stress-parameter types in turn.

(1) Guidelines for maximum energy release rate

The maximum energy release rate criterion considers that the idea of crack expansion can be considered from the point of view of energy release, and this criterion has two basic assumptions: the crack begins to expand when the maximum energy release rate reaches a critical value, and the crack expands in the direction of the maximum energy release rate generated by the crack tip. This fracture criterion is related to the fact that, by derivation, the maximum energy release rate is obtained as follows.

$$G_{\min} = \frac{1+\nu^2}{E} k^2. \tag{1}$$

(2) Minimum strain energy density criterion

Similarly, the basic assumption of this fracture criterion is that crack expansion along the direction of minimum strain energy density is associated with it reaching a critical. The minimum strain energy can also be obtained by analogous reasoning.

$$s(\theta) = c \cdot S_{\min}, \tag{2}$$

$$S_{\min} = \frac{1+2\nu}{2\pi s} k. \tag{3}$$

This chapter aims to architect a fully automated statistical analysis system for structural surface parameters based on digital image processing techniques. The choice of "fully automated" as the research objective makes the elimination of manual intervention an important consideration in the

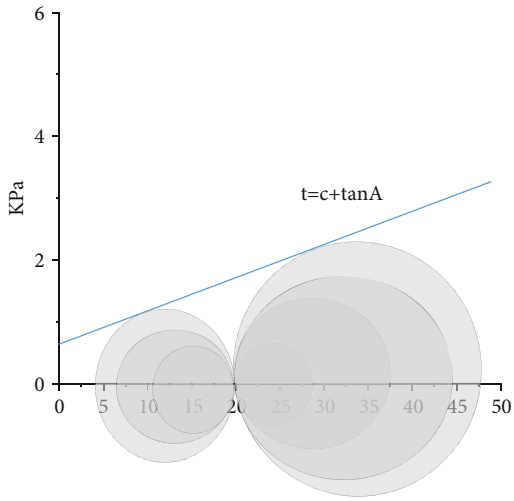

Figure 1: Mohr stress circle.

development process. The loading failure process is equivalent to the external energy input to the rock mass, and for the rock mass with a certain in situ stress field, there is residual strain energy during it. The excavation and unloading of the rock mass are a process of energy release, which leads to changesin the mechanical properties completeness of the rock mass..

A digital camera is first used to image the unsupported roof face, followed by image preprocessing with local histogram equalization, adaptive gamma correction, and median filtering, then, the structural face contour is extracted by area growth segmentation and Hough transform, and the structural face skeleton is obtained by contour refinement and interrupted point connection, and finally, the structural face characteristic parameters are calculated and the GSI rating is calculated. The flow of the digital image analysis system is shown in Figure 2.

A Go-Pro digital camera (model: CHDHX-601-RW) was used for image acquisition. This digital camera has excellent waterproof, dustproof, and impact resistance properties, which is conducive to image acquisition in underground coal mines and meets the needs of posttesting. The camera lens is placed in the vertical direction of the rock face during the shooting process, which can avoid the image distortion caused by the angle error during the inclined shooting process. When the open-pit mine slope is excavated and exposed, the original ground stress balance is broken, and the rock slope tends to move to a stable state. At this time, its mechanical state is mainly shown as unloading. The construction of the external dump site produced vertical compressive stress on the slope, that is, the rock slope was adjusted from the original in situ stress balance state to the tension and compression stress state. The lack of effective lighting equipment at the roadway excavation working face and a suitable light source is an extremely important part of the imaging system. The current light source for the camera can be divided into three categories: direct light source, diffuse light source, and reflective light source, the difference is whether the light in the process of propagation from the light source to the object changes direction, a simple schematic diagram is shown in Figure 3. Direct light from the light source directly to the object surface, direct light is very easy to cause uneven distribution of image brightness, in the imaging of uneven rock surface, and direct light will cause many high-contrast shadow areas, hindering the subsequent image processing work. Diffuse light travels through a translucent diffuse plate during propagation, causing light to be emitted irregularly in different directions. Diffuse light softens shadow areas in the image, and at high luminance, it is even possible to achieve shadow elimination. The reflected light reaches the object after it has been reflected by an opaque surface. Both reflective and diffuse light can soften the light, but additional reflective surface controls need to be added during implementation, adding to the complexity of the system. In addition, reflection attenuates light intensity, which is not conducive to imaging work in dark environments.

2.2. Sensor Testing Technology Research. A wireless sensor network is a network system consisting of many intelligent sensor nodes deployed in a monitoring area, whose purpose is to collaboratively sense, collect, and process information about the sensed objects in the network coverage area. Compared with traditional monitoring methods, wireless sensor networks have the following advantages: (1) wireless communication. Therefore, scholars put forward fracture mechanics on this basis. Fracture mechanics is an important theoretical basis for analyzing the strength and life prediction of engineering materials and components. It is to study the balance, growth, and instability of cracks in components with cracks under the action of external forces,which is a new discipline of law and intensity. Smart sensor nodes are wirelessly connected and self-organized communication networks, which brings great convenience to instrument installation and greatly reduces installation cost and installation workload; (2) large-scale network. Small size, flexible arrangement, and many sensor nodes can be deployed in the monitoring area to form a large-scale network, through different spatial perspectives to obtain information with greater signal-to-noise ratio, reducing the accuracy requirements of individual sensor nodes, making the system has a strong fault-tolerant performance; (3) scalability and robustness (relative stability). Wireless sensor networks have the advantages of self-organization and self-healing, and sensor nodes can be randomly arranged and nodes are automatically configured and managed to form a multihop wireless network. Therefore, new expansion nodes can be added to the network at will, with good scalability, when a node failure, other nodes automatically find a new transmission path, does not affect the normal work of the entire network, to ensure the overall network robustness; (4) have local computing and processing capabilities. Sensor nodes integrated microprocessor and memory can achieve self-calibration, self-diagnosis, and other functions, the original data processing, extraction of useful information, greatly reducing the amount of data to be transmitted wirelessly; (5) damage recognition and localization capabilities. Wireless sensor network that enables node localization. Combined with the structural state information measured by sensors, the

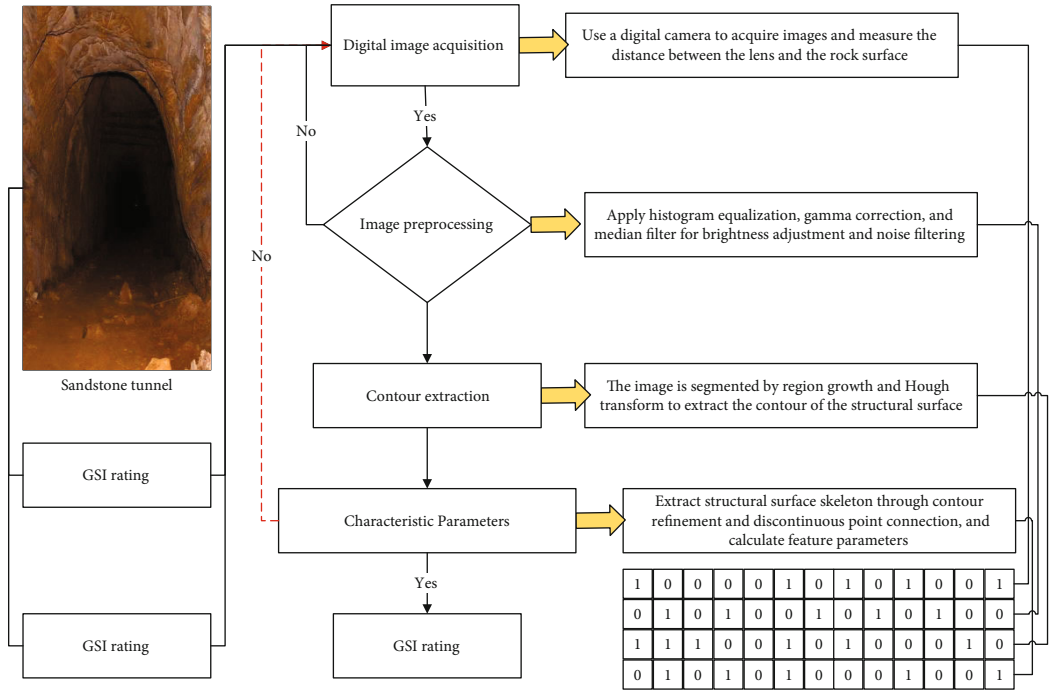

Figure 2: Flow chart of the digital image analysis system.

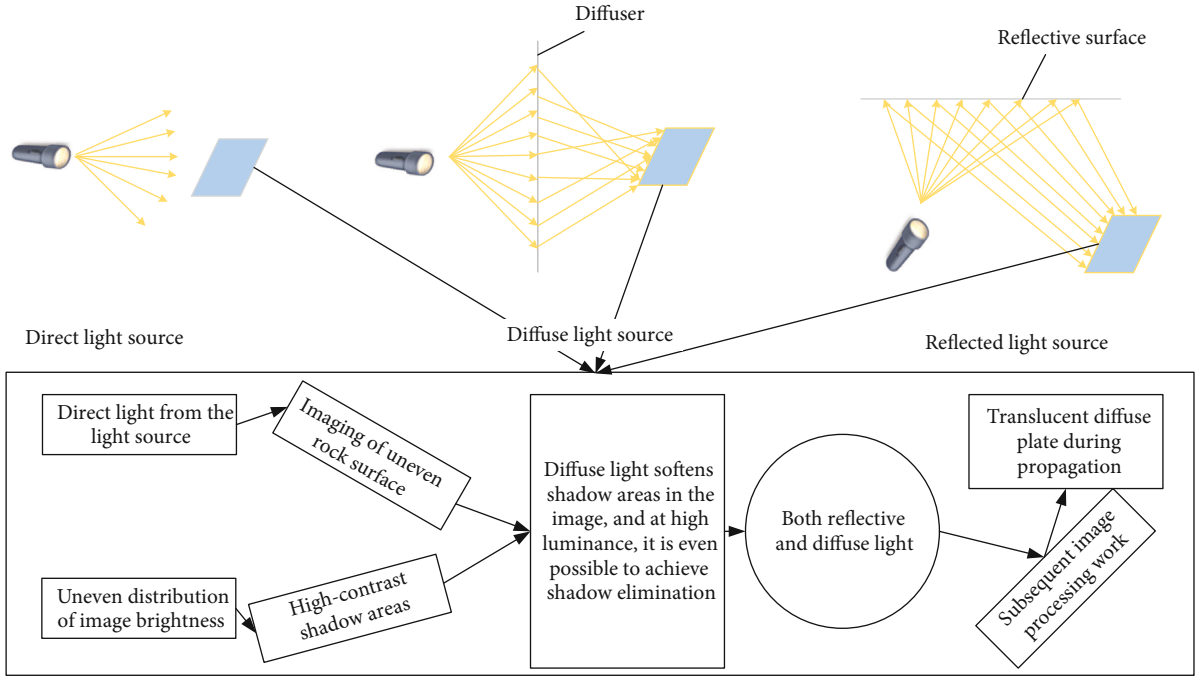

Figure 3: Schematic diagram of a direct light source, diffuse light source, and reflected light source.

damage recognition theory can be applied to automatically detect damage and accurately locate the damage location, which greatly promotes the intelligence of structural monitoring and maintenance.

At this stage, there are two types of inclination sensors, synchronous acquisition, and asynchronous acquisition, which in turn is important for deformation measurement. The method of achieving synchronization can be achieved by hardware and software methods, and the software method can be achieved by interpolation. The hardware synchronous acquisition technique is a bit-synchronous communication technique, and to achieve synchronization in hardware, the sender and receiver need to have clock signals of the same frequency and phase [17]. When no data

acquisition is required, the connection line is in MARK state. At the start of a measurement, the sender first sends one or two of the synchronization characters. Once both parties have achieved synchronization, large blocks of data can be sent in single character succession, thus, eliminating the need for start and stop bits. During transmission, both parties take a clock for coordination, which is used to determine the position of each bit in the serial transmission. The essential difference between compound cracks and single type cracks is that the cracking direction no longer extends along the original crack surface, but has a certain angle with it. Therefore, compound cracks need to determine the crack propagation angle based on a single crack. To start the measurement, both sides use the sync character to keep the clock internally synchronized with the sender, then the data following the sync character is shifted in bit by bit while converting to a parallel format for the CPU to read, and the data is not available until the end character is received. Synchronous acquisition uses a common clock, and synchronous acquisition has a high transmission frequency, to achieve high-speed, high-capacity data transmission. When data transmission is performed, both sides must maintain complete synchronization, requiring the receiving and sending devices to have the same clock and maintain strict synchronization. In summary, the system consists of a complete system topology consisting of a data processing platform on the server-side, a database station, and an inclination sensor, as shown in Figure 4.

To further analyze the characteristics of the open-loop and closed-loop structures, a mathematical model is developed to analyze both separately. First, the transfer function block diagram of the open-loop structure is established, where the voltage V is the out output of the system and the primary current Ip is the input of the system. b denotes the magnetic induction intensity generated by the primary current I in the paleomagnetic loop, and the coefficient K is used to define the relationship between Ip and Bp: $K =$ Bp/Ip. According to the ampere-loop theorem, K can also be expressed as

$$K = \frac{3u_0}{2d}. \tag{4}$$

The static gain SI (0) represents the sensitivity of the entire system, which is also the turn ratio of the primary coil to the feedback coil. Since the number of turns of the primary coil is generally 1, the turn ratio is determined by the number of turns of the feedback coil only. Therefore, when the number of turns of the feedback coil is certain, the feedback current is always proportional to the primary current even though the nonlinear error or temperature drift of the TMR sensor affects the open-circuit sensitivity coefficient Ka of the TMR sensor, which improves the measurement accuracy of the TMR current sensor, eliminates the offset and drift associated with the chip temperature, and greatly reduces the error caused by the hysteresis phenomenon. Based on the transfer function of the closed-loop TMR current sensor, the cutoff frequency of the system can be obtained as

$$f(0) = \frac{K_a + K_s + K_b}{2\pi R_{t0}}. \tag{5}$$

The cutoff frequency $f0$ indicates the bandwidth of the TMR current sensor, which is determined by the operational amplifier parameters τA, Ka, the feedback magnetic field coefficient Kb, the open-loop sensitivity coefficient Ks, and the feedback resistance Rm. In practical design, due to the high sensitivity of the TMR chip, the bandwidth of the closed-loop TMR current sensor can be as high as MHz when a suitable feedback magnetic field coefficient K and feedback resistance Rm are selected some time, it should be ensured that the feedback resistance Rm is large enough to obtain a good output voltage resolution. Increasing the value of K allows a wider bandwidth of the closed-loop TMR current sensor, but at the same time, the size of the number of turns N of the feedback 2coil should be limited to ensure a good current sensitivity of the system. Compared with traditional monitoring methods, wireless sensor networks have the following advantages: (1) wireless communication. The use of wireless connection between intelligent sensor nodes and self-organizing communication network brings great convenience to the installation of the instrument, greatly reducing installation cost and installation workload; (2) large-scale network. Small size, flexible layout, and many sensor nodes can be deployed in the monitoring area to form a large-scale network, obtain information with greater signal-to-noise ratio through different spatial perspectives, reduce the accuracy requirements for a single sensor node, and make the system highly fault-tolerant performance; (3) scalability and robustness (relative stability). Wireless sensor networks have the advantages of self-organization and self-healing. Sensor nodes can be randomly arranged, and nodes can be automatically configured and managed to form a multihop wireless network. Therefore, new expansion nodes can be added arbitrarily in the network, which has good scalability. When a node fails, other nodes automatically find a new transmission path, which does not affect the normal operation of the entire network and ensures the robustness of the overall network nature; (4) have local computing and processing capabilities. The integrated microprocessor and memory of the sensor node can realize self-calibration, self-diagnosis, and other functions, process raw data, extract useful information, and greatly reduce the amount of data that needs to be wirelessly transmitted; (5) damage identification and location capabilities. Wireless sensor network can realize node positioning. Combining the structural status information measured by the sensors and applying the damage recognition theory can automatically detect damage and accurately locate the damage location, which greatly improves the detection accuracy.

The sensitivity of the TMR current sensor is low when using the single wire measurement model, and it is difficult to ensure that the relative positions of the wire and the TMR chip are fixed, so the effect of a change in the relative

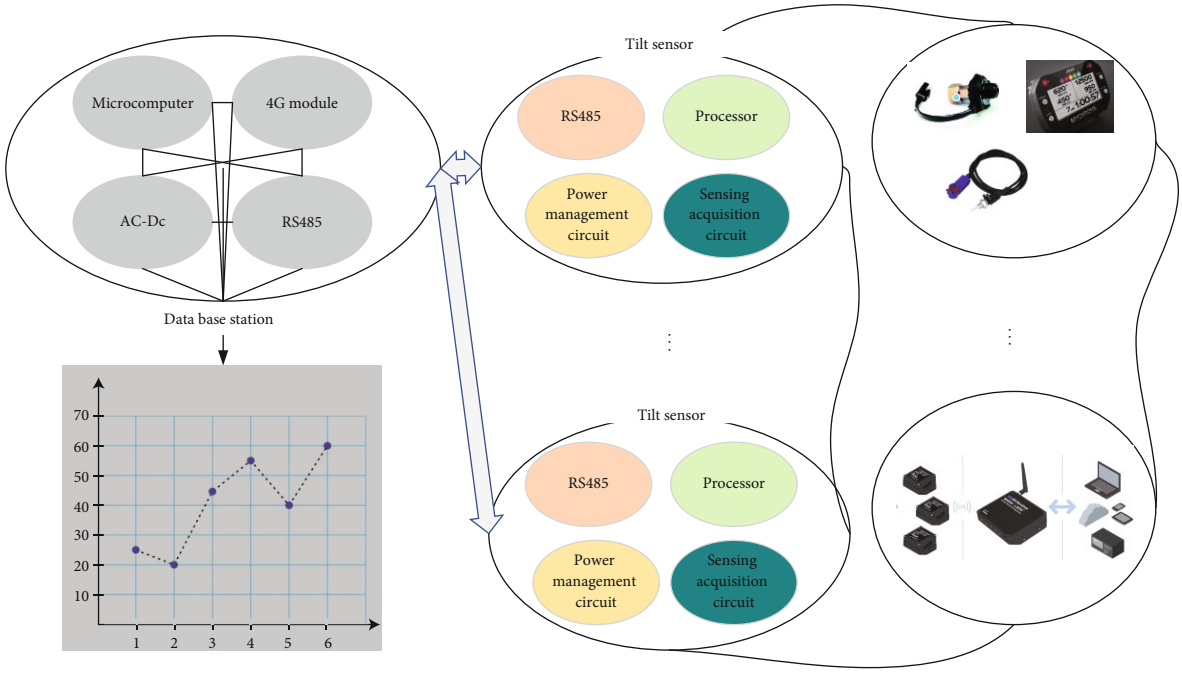

Figure 4: Sensor acquisition system topology diagram.

positions of the two on the measurement accuracy is further analyzed. The position of the wire is taken as the center of the circle, the TMR is the point on the circle, and the effect of the wire deviating from the center of the circle on the measurement is analyzed [18]. The simulation model is built in COMSOL simulation software, the radius of the wire is 5 mm, the length is 0.5 m, the size of the TMR chip is 0.8 mm × 5 mm × 3.5 mm, the distance between the TMR chip and the wire is $r0$ is 30 mm, and the magnetic field distribution at the TMR chip is analyzed at different positions of the wire. Since the magnetic sensitivity axis of the TMR chip is in the $+X$ direction, the magnetic flux on the surface of the TMR chip is used as a comprehensive measure of the magnetic field distribution at the TMR chip. The magnetic field distribution at the TMR chip is considered for the two cases of the wire moving along the $+X$ direction and the wire moving along the $+Y$ direction, respectively. Analyze the case of the wire moving along the $+X$ direction. As shown in Figure 5, the X-coordinate of the wire is changed so that the wire moves along the $+X$ direction. The X-coordinate of the wire is scanned parametrically with the X-coordinate ranging from -18 mm to 18 mm, and the wire is made to move 1 mm along the $+X$ direction each time to find the magnetic flux at the surface of the TMR chip.

3. Results and Analysis

3.1. Performance Testing of Sandstone Tunnel Cracking Model with Fracture Mechanics Theory. The rock is a highly typical nonhomogeneous rock mass, and the expansion and changes of its internal microjoint fractures are closely related to time. The deterioration process of the sloping rock in open-pit mines is a nonlinear cumulative process closely related to time, and the slope stability is typically time-dependent. During the whole cycle from open pit excavation, slope exposure to final backfill and burial, changes in the external environment, such as blasting vibration, mining disturbance, weathering, groundwater infiltration, frost, and cold shrinkage, may cause the destruction and accumulation of the internal microstructure of the rock, and with time, the mechanical strength of the rock body continues to decay and gradually converge to a low limit value of stable convergence, resulting in the overall stability of the slope. Therefore, it can be considered that the stability of slopes in open-pit mines is dynamic [19]. The external factors affecting the exposure time of slopes can be summarized in the following two major aspects: (1) synthetic mining disturbance factors. It is mainly reflected in the whole mining process system of the open-pit mine, including the perforation of coal rock near the slope, loose blasting vibration, and excavation and transportation of ore and soil discharge along with the gang. When there is no need to collect data, the connection line is in the MARK state. At the beginning of the measurement, the sender first sends one or two synchronization characters. When the two parties reach synchronization, they can continuously send large blocks of data with a single character, so that the start bit and stop bit are no longer needed. These operational processes will produce certain damage to the geotechnical body, and the degree of damage accumulation is closely related to the slope exposure time. (2) Natural environmental factors. Mainly reflected in the geotechnical body is located in the natural environment changes, the impact on the physical and mechanical properties, and strength of the slope geotechnical body, including groundwater level, temperature changes, rainfall erosion, and physical and chemical weathering. Take temperature change as an example, for the slope of the open-pit mine located in the seasonal freezing area, due to the

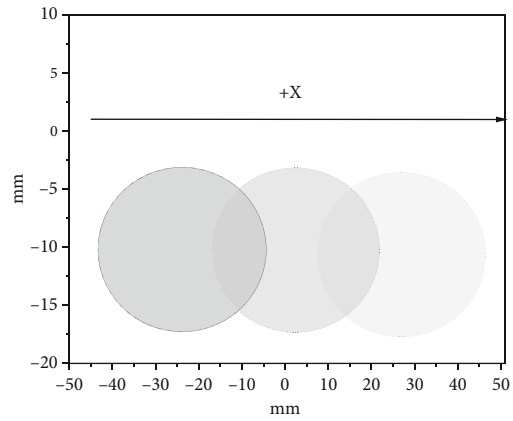

Figure 5: Simulation model of guidewire movement along +*X* direction (top view).

seasonal and temperature changes, the water in the slope constantly freezes and melts, changing the structure and distribution of the original joint fissures and weakening the stability of the slope.

$$t = \frac{(\cot \alpha - \cot \beta) - D}{v_p}. \tag{6}$$

The fracture behavior of a chambered and jointed rock mass can be considered as a complex flawed rock mass, which depends mainly on the emergence, extension, and agglomeration of cracks during loading. The fracture behavior of a rock mass containing a jointed chamber is closely related to the stress distribution around the chamber under the corresponding loading conditions. To gain insight into the damage pattern and crack evolution of the specimens from chambers containing parallel joints, it is necessary to first conduct a brief analysis of the stress distribution around the chamber. To facilitate the theoretical derivation, the chamber is usually simplified to a planar stress problem, the stress distribution around the chamber is calculated based on two-dimensional elastic theory for biaxial stress conditions, and the theoretical analysis model is shown in Figure 6.

To study the deformation evolution and crack extension process of composite defective rock specimens from a fine viewpoint, the image evolution characteristics of the specimens during deformation and damage were recorded by a digital image correlation system, and after postprocessing, the change characteristics of deformation fields (displacement field and strain field) during deformation and damage of the specimens were obtained, and then the crack extension evolution law of the specimens at different stress stages under static load was analyzed and compared [20]. Changes in the external environment, such as blasting vibration, mining disturbance, weathering, groundwater infiltration, frost heave, and cold shrinkage, may cause the damage and accumulation of the fine structure of the rock. As time goes by, the mechanical strength of the rock mass continues attenuation and gradually approaching a stable and convergent low limit value, resulting in a gradual decrease in the overall stability of the slope. Therefore, it can be considered that the slope stability of the open-pit mine changes dynamically. Due to the high strength of the composite defective rock material used in this paper, the deformation field on the surface of the specimen does not change significantly in the preloading stage, and the obvious crack extension phenomenon generally occurs only in the stable crack extension stage and the unstable crack extension stage. Therefore, according to the development characteristics of the stress-strain curve of the specimen and combined with the evolution characteristics of AE events, some key stress points of the specimen in the crack stable extension stage and the crack unstable extension stage are selected to analyze the evolution characteristics of the deformation field.

The results of the NMR analysis show that the sandstone, the concrete side, and the interface have significantly different pore distribution evolution patterns under the freeze-thaw action. The sandstone and the interface show variation characteristics that are distinct from those of single materials. In contrast, sandstone near the interface is more susceptible to the effects of interfacial action. This chapter focuses on the effect of the presence of interface on the sandstone side and refers to it as Interface Influence Zone (IIZ). The extent of the interface influence zone is further identified and related to different freeze-thaw environments, and the evolutionary mechanism of the interface influence zone is explored from a fine-scale perspective. Based on the NMR signal intensity, the pore volume of the sandstone part is much larger than that of the concrete part. For the initial state, i.e., 0 freeze-thaw cycles, the sandstone-concrete binary exhibits a significant difference along the longitudinal direction. This phenomenon can be attributed to the original individual variability within the test. The NMR signal intensities at different numbers of freeze-thaw cycles are considered in conjunction with the NMR signal intensities at 0 freeze-thaw cycles. At the 14–17-layer position, i.e., within 13.6 mm of the interface in the sandstone, the freeze-thaw effect on the NMR signal is evident. In this range, the NMR signal intensity increases by about 50,000 a.u. with an increasing number of freeze-thaw cycles. However, at other locations in the sandstone-concrete diatom, the NMR signal intensity changes less. This analysis shows that under the effect of freeze-thaw cycles from -10°C to 10°C, the sandstone portion near the interface (layers 14-17) shows significant pore volume changes, exhibiting significant water aggregation and water migration to the interface. To deeply understand the failure mode and crack evolution of the chamber sample of rock mass with parallel joints, it is necessary to briefly analyze the characteristics of the stress distribution around the chamber. To facilitate theoretical derivation, the chamber is usually simplified as a plane stress problem, and the stress distribution around the chamber under biaxial stress conditions is calculated based on the two-dimensional elastic theory.

Analyzed at the interface, the interface is the cemented surface of the sandstone and concrete, and an interfacial transition zone is formed at the interface. The hydration of the cement in the part of the interface transition zone is

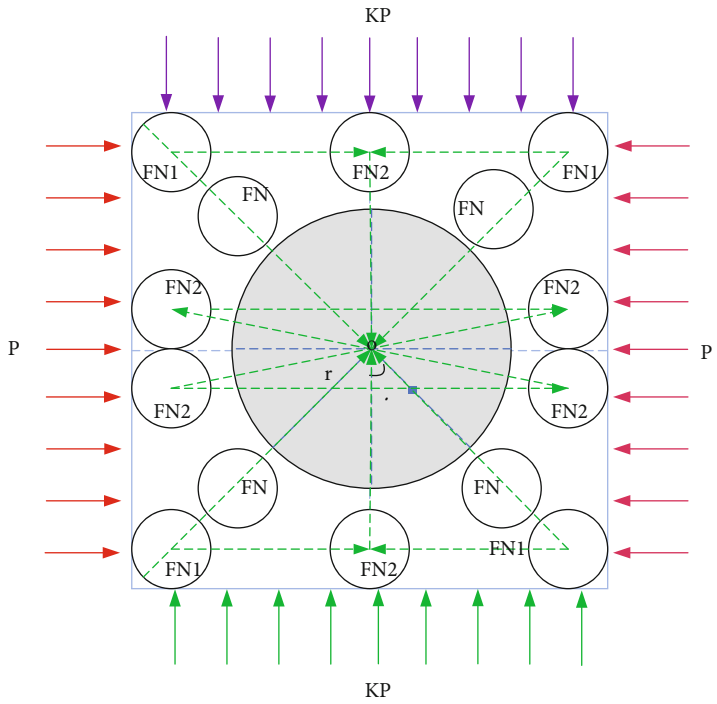

Figure 6: Simplified diagram of the stress distribution in the plane of the chamber under stress conditions.

different from the interior of the concrete. The interfacial transition zone is distributed with more calcium alumina crystals, and the interfacial fracture toughness is low. It should be noted that the interface transition zone has less distribution of both pores due to the intrusion of cement at the interface. However, at the same time, based on the pore distribution, a small number of large pores occur at the interface. Therefore, the analysis suggests that at the beginning of the freeze-thaw cycle, the hydraulic fracturing phenomenon mainly arises within the interface-influenced zone. The freeze-swelling force is not yet sufficient to cause fracture extension at the interface, or there are few newborn fractures at the interface part relative to the sandstone end. The water pressure inside the pore space is sufficient to crack the interface under repeated freeze-thawing action. And after the interface cracking, the later freeze-thawing has more influence on the interface cracking because the large pores of the interface have penetration, and the internal water pressure is more easily released along with the interface.

The extent of the interfacial zone of influence varies at different temperature intervals. At relatively high temperatures, the range of the interface influence zone is larger; at lower temperatures, the range of the interface influence zone is smaller. This phenomenon can be attributed to the combined effect of interface and freezing temperature. As shown in Figure 7, for low freezing temperature, the freeze swell force curve shows an increase and then a decrease, and there is a peak freeze swell force; for low freezing temperature, the same is true for the freeze swell force. However, for the low freezing temperature state, it produces a larger freeze swell force. In the sandstone near the interface, the low freezing temperature causes damage and cracking of the sandstone more easily and quickly. However, based on the test results, the low freezing temperature does not produce an increased area of influence at the interface under multiple freeze-thaw cycles.

3.2. Results of Sensor Testing Techniques. The static characteristics of the TMR current sensor mainly include sensitivity, range, linearity, accuracy, and other parameters, which must be calibrated before using the TMR current sensor. The TMR current sensor was sent to the Municipal Institute of Metrology and Quality Inspection for testing and calibration, and the testing equipment was a special clamp meter calibration device and a digital multimeter of type 8846A. The input and output curves of the TMR current sensor can be obtained by changing the current of the clamp meter calibration device and recording the corresponding output voltage of the TMR current sensor at different currents. The sensitivity of the sensor is defined as the ratio of the increment of the output quantity to the corresponding increment of the input quantity that causes the increment, so the sensitivity of the TMR current sensor is the ratio of the change of the output voltage to the change of the measured current. The current test range was first set to -60 A to 60 A, and the data from the test was imported into the origin plotting software for a linear fit, and the input and output curves were drawn as shown in Figure 8. The black curve is the input and output curve of the open-loop TMR current sensor, and the red curve is the input and output curve of the closed-loop TMR current sensor.

The maximum deflection error between the inclination sensor and the measured deformation curve of the total

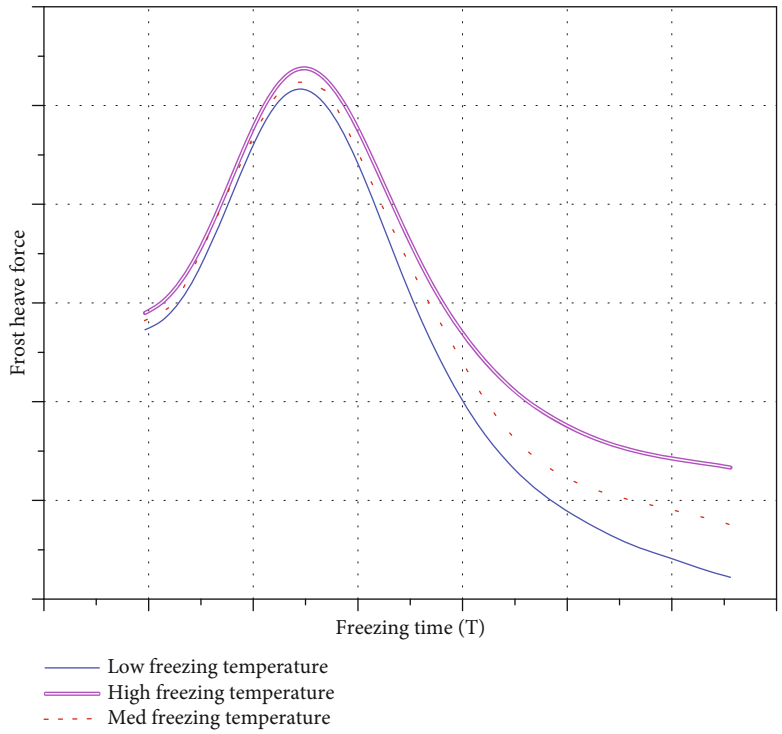

Figure 7: Schematic diagram of the development of internal freezing and swelling forces in sandstone at different freezing temperatures.

station is 0.7 mm, and the difference in the deformation curve is not significant. The inclination sensor for measuring tunnel deflection has the following advantages.

(1) The tilt sensor is small and easy to carry. Its size is 120 mm∗150 mm∗40 mm, which can be carried in large quantities band

(2) The inclination sensor is easy to install, the measuring point is not easy to damage, the aluminium housing can guarantee its long-term use, and not subject to measurement conditions, it can be used in unlit conditions

(3) Inclination sensors are less costly instruments compared to total stations and can be recycled

(4) The inclination sensor has high testing accuracy, and the measured inclination can be up to 9 decimal places, while the total station measures the deflection values can only be measured to an accuracy of two decimal places

(5) Inclination sensors can be realized in the office under the premise of unattended, real-time monitoring can be achieved. Using the user platform, through the computer control, you can achieve real-time monitoring, greatly reducing the workload, as well as the test time on site. And the tilt sensor acquisition can be achieved high frequency, that is, 1 s acquisition of 20, 50, and 100 numbers, real-time monitoring. This chapter introduces the application of the inclination sensor in the subway deformation monitoring

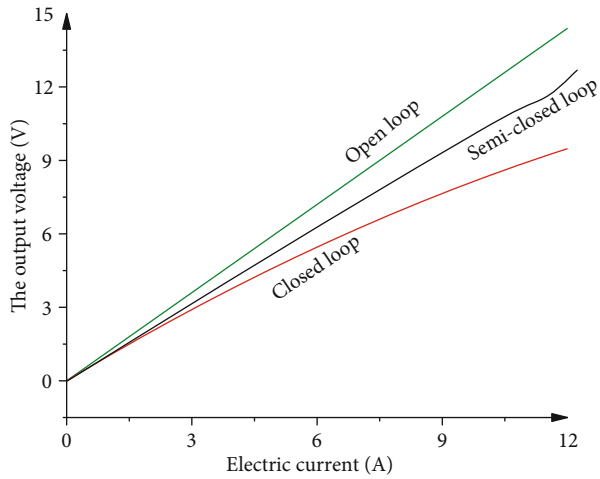

Figure 8: Input and output curves for open-loop and closed-loop structures.

example, through the inclination sensor and the total station measured data with the theoretical curve for comparison and analysis, know the inclination sensor and the total station measured data deformation curve difference is not large, the inclination sensor applied to the tunnel deformation measurement is feasible. The data in this chapter show that the maximum deflection value measured by the inclination sensor is 1.86 mm, which is less than the theoretically calculated value of 8.23 mm and less than the warning value of 10 mm, and the existing tunnel will be affected by the tunnel excavation, but overall, it is

safe. Compared with the traditional total station monitoring method, the inclination sensor has several advantages such as small size, easy installation, high testing accuracy, and realizing real-time monitoring

4. Conclusion

The development and utilization of underground space are an inevitable choice for human social development, economic construction, and strategic security needs. As a nonlinear, noncontinuous, nonhomogeneous, and anisotropic natural geological body, the rock body is randomly distributed with discontinuous structural surfaces such as joints, fractures, weak interlayers, and faults of different scales inside after a long period of geological action. The mechanism of rock instability damage and its stability and control problems is some of the key scientific problems that are currently focused on and urgently need to be solved in the field of rock mechanics. Compared with traditional wired monitoring methods, wireless sensor networks can overcome many drawbacks of traditional wired monitoring methods and have obvious advantages in many aspects such as instrument installation, data measurement, condition assessment, and cost control, which provide convenience for health monitoring work and are the future development direction of structural health monitoring. This paper discusses the model of sandstone tunnel cracking based on fracture mechanics theory with the help of sensor testing technology, and some results have been achieved. However, due to the complexity of sandstone tunnels themselves and the environment, there are very few studies dedicated to the application of wireless sensor networks in the intelligent monitoring of sandstone tunnels. The actual geography of sandstone tunnels is more complex, and further research work is still needed for a comprehensive analysis of their interface debonding characteristics. Therefore, a more in-depth study on the application of wireless sensor networks in tunnelling is of great significance for both human society and economic development.

Data Availability

The data used to support the findings of this study are available from the corresponding author upon request.

Conflicts of Interest

The authors declare that they have no known competing financial interests or personal relationships that could have appeared to influence the work reported in this paper.

Acknowledgments

The study was supported by Southwest Jiaotong University.

References

[1] F. Zhao, Z. Shi, and Q. Sun, "Fracture mechanics behavior of jointed granite exposed to high temperatures," *Rock Mechanics and Rock Engineering*, vol. 54, no. 5, pp. 2183–2196, 2021.

[2] W. Guo, F. Yu, Y. Tan, and T. B. Zhao, "Experimental study on the failure mechanism of layer-crack structure," *Energy Science & Engineering*, vol. 7, no. 6, pp. 2351–2372, 2019.

[3] L. Zhang, D. Yang, Z. Chen, and A. Liu, "Deformation and failure characteristics of sandstone under uniaxial compression using distributed fiber optic strain sensing," *Journal of Rock Mechanics and Geotechnical Engineering*, vol. 12, no. 5, pp. 1046–1055, 2020.

[4] X. Fu, Y. X. Ban, Q. Xie, R. A. Abdullah, and J. Duan, "Time delay mechanism of the Kaiser effect in sandstone under uniaxial compressive stress conditions," *Rock Mechanics and Rock Engineering*, vol. 54, no. 3, pp. 1091–1108, 2021.

[5] J. Chen, J. Zhao, S. Zhang, Y. Zhang, F. Yang, and M. Li, "An experimental and analytical research on the evolution of mining cracks in deep floor rock mass," *Pure and Applied Geophysics*, vol. 177, no. 11, pp. 5325–5348, 2020.

[6] D. Liu, K. Ling, D. Li et al., "Evolution of anisotropy during sandstone rockburst process under double-faces unloading," *Journal of Central South University*, vol. 28, no. 8, pp. 2472–2484, 2021.

[7] Y. H. Huang, S. Q. Yang, and J. P. Dong, "Experimental study on fracture behaviour of three-flawed sandstone specimens after high-temperature treatments," *Fatigue & Fracture of Engineering Materials & Structures*, vol. 43, no. 10, pp. 2214–2231, 2020.

[8] P. Zhou, J. Li, Y. Jiang et al., "Damage mechanism of tunnels in the high-content salt rock stratum," *Bulletin of Engineering Geology and the Environment*, vol. 80, no. 10, pp. 7633–7652, 2021.

[9] C. Niu, Z. Zhu, F. Wang, P. Ying, and S. Deng, "Effect of water content on dynamic fracture characteristic of rock under impacts," *KSCE Journal of Civil Engineering*, vol. 25, no. 1, pp. 37–50, 2021.

[10] Q. Xie, S. Li, X. Liu, F. Q. Gong, and X. B. Li, "Effect of loading rate on fracture behaviors of shale under mode I loading," *Journal of Central South University*, vol. 27, no. 10, pp. 3118–3132, 2020.

[11] W. Yu, G. Wu, B. Pan, Q. Wu, and Z. Liao, "Experimental investigation of the mechanical properties of sandstone–coal–bolt specimens with different angles under conventional triaxial compression," *International Journal of Geomechanics*, vol. 21, no. 6, 2021.

[12] Y. Zhang, X. Yao, P. Liang et al., "Fracture evolution and localization effect of damage in rock based on wave velocity imaging technology," *Journal of Central South University*, vol. 28, no. 9, pp. 2752–2769, 2021.

[13] H. Wu, B. Dai, L. Cheng, R. Lu, G. Zhao, and W. Liang, "Experimental study of dynamic mechanical response and energy dissipation of rock having a circular opening under impact loading," *Mining, Metallurgy & Exploration*, vol. 38, no. 2, pp. 1111–1124, 2021.

[14] A. Sedmak, "Computational fracture mechanics: an overview from early efforts to recent achievements," *Fatigue & Fracture of Engineering Materials & Structures*, vol. 41, no. 12, pp. 2438–2474, 2018.

[15] X. Li, F. Gong, M. Tao et al., "Failure mechanism and coupled static-dynamic loading theory in deep hard rock mining: a

review," *Journal of Rock Mechanics and Geotechnical Engineering*, vol. 9, no. 4, pp. 767–782, 2017.

[16] X. Zhang, Z. Li, E. Wang, B. Li, J. Song, and Y. Niu, "Experimental investigation of pressure stimulated currents and acoustic emissions from sandstone and gabbro samples subjected to multi-stage uniaxial loading," *Bulletin of Engineering Geology and the Environment*, vol. 80, no. 10, pp. 7683–7700, 2021.

[17] Z. Jinhao, C. Hongkai, W. He, and Z. Zheng, "Experimental study on damage evolution characteristics of rock-like material," *Arabian Journal for Science and Engineering*, vol. 44, no. 10, pp. 8503–8513, 2019.

[18] K. Zhang, X. Liu, Y. Chen, and H. Cheng, "Quantitative description of infrared radiation characteristics of preflawed sandstone during fracturing process," *Journal of Rock Mechanics and Geotechnical Engineering*, vol. 13, no. 1, pp. 131–142, 2021.

[19] S. Fereshtenejad, J. Kim, and J. J. Song, "The effect of joint roughness on shear behavior of 3D-printed samples containing a non-persistent joint," *Petrophysics-The SPWLA Journal of Formation Evaluation and Reservoir Description*, vol. 62, no. 5, pp. 553–563, 2021.

[20] L. Li, Y. Liu, W. Liu et al., "Crack evolution and failure modes of shale containing a pre-existing fissure under compression," *ACS Omega*, vol. 6, no. 39, pp. 25461–25475, 2021.